Hindawi
Shock and Vibration
Volume 2019, Article ID 5169156, 14 pages
https://doi.org/10.1155/2019/5169156

Research Article

Dynamic Characteristics Analysis of Marine Propulsion Shafting Using Multi-DOF Vibration Coupling Model

Yuanchao Zhang,[1,2] Wei Xu,[1,2] Zhengmin Li,[1,2] Jiangyang He,[3] and Lihang Yin[1,2]

[1]*Naval University of Engineering, Institute of Noise & Vibration, Wuhan, China*
[2]*National Key Laboratory on Ship Vibration & Noise, Wuhan, China*
[3]*Navy Submarine Academy, Qingdao, China*

Correspondence should be addressed to Zhengmin Li; lizhengm100@163.com

Received 20 June 2019; Revised 6 September 2019; Accepted 17 September 2019; Published 25 November 2019

Academic Editor: Franck Poisson

This paper mainly focuses on the elastic support of thrust bearings. The dynamic characteristics of the shafting system are studied. Firstly, the multi-DOF transfer matrix expressions of the simplified mass element and spring element are derived. A three-DOF transfer matrix-coupling model in *XOZ* plane is established by using force coupling conditions at thrust bearings. Then, a test rig is built to test the propulsion shafting. The bending vibration characteristics of the shafting under the support conditions of thrust bearings are studied. And finally, the transmission characteristics of vertical and longitudinal forces of propellers under different support conditions of thrust bearings are emphatically analyzed.

1. Introduction

The mechanical noise of marine stern has always been the focus of attention in the field of vibration reduction and noise reduction in various countries [1]. The large propulsion machine of the stern is the main noise source [2]. When the vibration of power equipment is well controlled, the propulsion shafting of the stern becomes the main factor affecting noise.

The alternating thrust generated by the propeller rotating in the stern is the main source of excitation for the longitudinal vibration of the propulsion shafting system. The force of the blade changes periodically every turn, and the force of the propeller changes periodically with z_p (z_p is the number of blades). Therefore, the basic frequency of the alternating thrust is blade frequency, and the frequency of its high-order harmonics is integer multiples of blade frequency [3]. In addition, the unbalanced mass of the propeller caused by inadequate manufacturing accuracy will generate dynamic unbalanced force when the shafting is running, which is also an effective excitation to the longitudinal vibration of the shafting, and the corresponding frequency is the shaft frequency [4].

After mastering the excitation characteristics and hazards of propulsion shafting vibration, scholars all over the world have carried out a wealth of research on the transmission mechanism of longitudinal vibration of shafting through propulsion shafting. Pan et al. [5] studied the problem comprehensively and built a small test rig, as shown in Figure 1. The test results show that the transmission characteristics of propulsion shafting are quite different under different working conditions. The parameters of propulsion shafting are nonlinear under rotational speed and load. The parameters of propulsion shafting have a great influence on the longitudinal vibration characteristics of shafting.

Based on Pan's research results, Xie et al. [6] has carried out theoretical and experimental research on the transmission characteristics of the shafting subsystem by using the marine berthing stage. The longitudinal stiffness parameters of propulsion shafting are emphatically tested and compared with the theory.

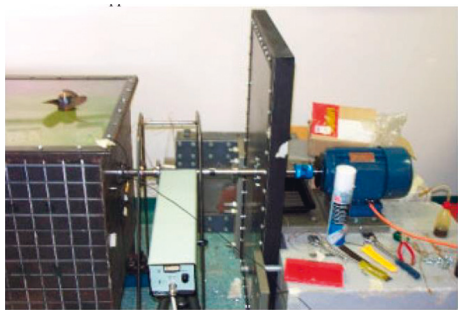

Figure 1: Test rig used by Pan [5].

Zhang et al. [7–10] and others have carried out relevant theoretical research on the longitudinal vibration of shafting and also pointed out that the longitudinal stiffness parameters of propulsion shafting are the main parameters affecting the longitudinal vibration of shafting. A kind of propulsion shafting with hydraulic vibration reduction is presented, as shown in Figure 2. Principle prototype verifies the control effect. In order to simulate the elasticity of submarine shell, Li et al. [11] built a scaled model test rig and carried out theoretical and experimental research on this problem. The influence of oil-film stiffness characteristics of propulsion shafting on the longitudinal vibration of the shafting is studied. According to Pan's research results, an active control algorithm is designed, but no new test results are published. On this basis, the relevant control measures are put forward in [12, 13], but there are still some problems, such as the theoretical design is too complex and the control algorithm is not mature. Mead and Yaman [14, 15] put forward the wave theory to study the longitudinal vibration characteristics of shafting. It has clear physical meaning and complete analytical solution to analyze the longitudinal vibration characteristics of shafting with theoretical solutions of one-dimensional wave equation under different boundary conditions. Zhou and Yi [16] applied this method to analyze the longitudinal vibration characteristics of marine propulsion shafting under different support systems. It is pointed out that the stiffness of propulsion shafting is the main factor affecting the longitudinal vibration characteristics of the shafting. Zhang and Zhao [7] also applied this method to the multistep structure of marine shafting with variable cross section. The continuity condition at variable cross section is proposed to simplify the shafting into a uniform shaft. The detailed characteristic frequency equation of the longitudinal vibration of the shafting is deduced, and the influence trend of the stiffness value of propulsion shafting on the vibration characteristics of the shafting is analyzed. Zou et al. [17] established a nonlinear coupled longitudinal-transverse dynamic model of the marine propulsion shafting and investigated the transverse superharmonic resonances under blade frequency excitation. Zou et al. [18] studied the oil-film stiffness and composite support stiffness of the thrust bearing in marine

Figure 2: The experimental rig for marine propulsion shafting longitudinal vibration [7–10].

propulsion shafting. The method of measurement for the oil-film stiffness and the composite support stiffness is investigated, and the experiment is carried by this method in a scaled thrust bearing test rig. Aiming at the problem of radiated noise caused by low frequency vibration of the tail of low speed ship, the longitudinal vibration of shafting is taken as the starting point. He et al. [19] established the theoretical model of the longitudinal vibration of the shafting by using the theory of structural elastic wave, deduced the characteristic frequency equation of the longitudinal vibration of the shafting in detail, and analyzed the attenuation effect of the integrated vibration isolation system and RC support subsystem on the longitudinal vibration of the shafting.

In order to effectively reduce the natural frequency of the longitudinal vibration of the shafting, most of the used thrust bearings are supported by elastic support [20], but this support system changes the vibration state of other DOF. The thrust bearing with elastic support will affect the state of marine propulsion shafting. However, the dynamic characteristics of the propulsion shafting will affect the marine vibration and noise. For the existing integral vibration isolation system, the arrangement of isolators often fails to realize the six-DOF decoupling of the stiffness matrix of the vibration isolation system, and there is a common phenomenon of multi-DOF coupling. Therefore, it is particularly important to study the dynamic characteristics of thrust bearing elastic support shafting. In this paper, theoretical and experimental studies will be carried out.

The innovative contributions of this paper can be summarized as follows:

(1) Considering the elastic supporting of the thrust bearing, a three-DOF transfer matrix-coupling model in the *XOZ* plane is established.

(2) The experiments of shaft bending under two supporting conditions are designed and carried out. In addition, the bending vibration characteristics of shafting are analyzed.

(3) The transmission characteristics of vertical force and longitudinal force under different conditions are analyzed.

The rest of this paper is organized as follows: Section 2 briefly introduces the three-DOF transfer matrix-coupling model. The design process of the test is detailed in Section 3. In Section 4, the vibration characteristics of the shafting system are briefly described. Section 5 provides a description of longitudinal and vertical transfer characteristics. Finally, conclusions are drawn in Section 6.

2. Multi-DOF Vibration Coupling Model of the Shafting System

Marine shafting vibration is a complex vibration system with great specificity and time varying and many influencing factors. Generally, according to the six-DOF in Cartesian coordinate system, marine shafting vibration can be divided into gyration vibration, longitudinal vibration, and torsional vibration. Longitudinal vibration and torsional vibration include single-DOF, while gyration vibration refers to the rotation of the shafting system around the deflection curve on the one hand and around the support center on the other hand, as shown in Figure 3, including four-DOF in the vertical and horizontal planes. The main reason for the gyro vibration is that the momentum vector caused by the polar moment of inertia and the radius moment of inertia of the rotating body changes constantly during the operation of the shafting, which has a great influence on the vibration characteristics of the shafting. The momentum moment is also called gyroscopic moment.

Because of the unbalanced mass of the shafting itself, the complex lubrication characteristics of the bearing and the different orientations of the cross section inertia parameters, the shafting multi-DOF coupling vibration forms are often caused. This paper studies the influence of the whole system on the shafting vibration characteristics after the propulsion shafting is supported by an elastic support, so it is necessary to make some assumptions about the shafting.

(1) Ignoring the gyroscopic effect of the shaft element

(2) Shaft element is an ideal element, ignoring shear deformation and unbalanced mass

(3) Ignoring the nonlinearity and mutual coupling of the bearing lubrication system, it is simplified as a single-point linear spring support in the horizontal and vertical planes

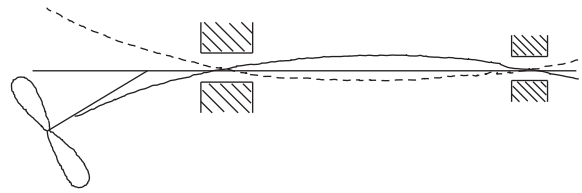

Figure 3: Schematic diagram of shafting whirling vibration.

(4) Ignoring the increase of deflection of the shaft element under pressure leads to the increase of bending stiffness

Based on the concentric support of radial bearings in each direction, the gyration vibration can be decomposed into the bending vibration in the vertical plane and the horizontal plane. Considering that the external load is mainly longitudinal force and the arrangement of isolator is limited, the coupling of the longitudinal DOF x with the vertical DOF z and the rotational DOF beta around the Y-axis of the isolation system can easily be formed. At the same time, the elastic support of the thrust bearing mainly changes the radial stiffness at the installation position of the thrust bearing and does not affect the torsional vibration characteristics of the shafting. Therefore, the integral vertical plane vibration isolation system is mainly analyzed. Coupled vibration characteristics with longitudinal bending of shafting, i.e., three-DOF coupling characteristics in the XOZ plane, the bending in this paper refers to the vertical plane bending, and the horizontal plane bending can be analogous to the vertical plane.

In this paper, the shafting system can be divided into mass element, shaft segment element, and spring element. Before listing the transfer matrix expression of each element, the positive direction of the element is first specified. Taking mass element as an example, it can be used for reference by other elements.

The force vector directions of the left and right ends of the element are shown in Figure 4. The axial direction is x, and the forward direction is from the bow to the stern; the vertical direction is z, and the vertical direction is positive; the vertical paper facing inward is y-axis. The expression of bending vibration of each element is given.

Quality components:

$$T_m = \begin{bmatrix} 1 & 0 & 0 & 0 \\ 0 & 1 & 0 & 0 \\ 0 & -J_d\omega^2 & 1 & 0 \\ m\Omega^2 & 0 & 0 & 1 \end{bmatrix}. \quad (1)$$

Shaft element:

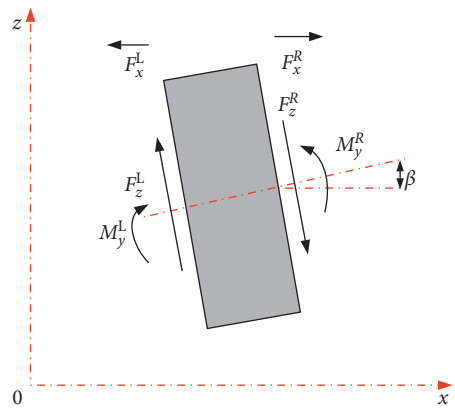

Figure 4: Schematic diagram of the positive direction of the end-state vector of the mass element.

$$T_s = \begin{bmatrix} \frac{\cos \beta L + ch\beta L}{2} & \frac{\sin \beta L + sh\beta L}{2\beta} & \frac{ch\beta L - \cos \beta L}{2EI\beta^2} & \frac{sh\beta L - \sin \beta L}{2EI\beta^3} \\ \frac{\beta(sh\beta L - \sin \beta L)}{2} & \frac{\cos \beta L + ch\beta L}{2} & \frac{sh\beta L + \sin \beta L}{2EI\beta} & \frac{ch\beta L - \cos \beta L}{2EI\beta^2} \\ \frac{EI\beta^2(ch\beta L - \cos \beta L)}{2} & \frac{EI\beta(sh\beta L - \sin \beta L)}{2} & \frac{\cos \beta L + ch\beta L}{2} & \frac{\sin \beta L + sh\beta L}{2\beta} \\ \frac{EI\beta^3(\sin \beta L + sh\beta L)}{2} & \frac{EI\beta^2(ch\beta L - \cos \beta L)}{2} & \frac{\beta(sh\beta L - \sin \beta L)}{2} & \frac{\cos \beta L + ch\beta L}{2} \end{bmatrix}. \quad (2)$$

Radial bearing spring elements:

$$T_k = \begin{bmatrix} 1 & 0 & 0 & 0 \\ 0 & 1 & 0 & 0 \\ 0 & 0 & 1 & 0 \\ -k_{rb} & 0 & 0 & 1 \end{bmatrix}. \quad (3)$$

The bending vibration transfer matrix and the longitudinal vibration transfer matrix of the above components are written in the form of a diagonal matrix.

Quality components:

$$T_m = \begin{bmatrix} T_{m-\mathrm{L}} & \\ & T_{m-\mathrm{B}} \end{bmatrix}. \quad (4)$$

Shaft element:

$$T_s = \begin{bmatrix} T_{s-\mathrm{L}} & \\ & T_{s-\mathrm{B}} \end{bmatrix}. \quad (5)$$

Spring element:

$$T_{rb} = \begin{bmatrix} I_{\mathrm{L}} & \\ & T_{rb-\mathrm{B}} \end{bmatrix}. \quad (6)$$

The angular scales L and B represent the longitudinal and bending vibrations, respectively; IL is a 2×2 unit matrix. The column vectors representing the state vectors at both ends of the element are 6×1, including three-DOF of axial displacement x, vertical deflection Z, and rotation beta around y-axis.

Observing the above transfer matrices, it can be found that under the assumption of ignoring the DOF coupling caused by the shafting, the transfer matrices mentioned above only write the longitudinal (2×2) and bending (4×4) columns of each element into the total transfer matrix (6×6) and do not have the coupling relation. The coupling relation between the isolation system and the longitudinal bending of the shafting is determined by using the force coupling condition at the thrust bearing with the elastic support.

As shown in Figure 5, for the traditional thrust bearing installation method, the hull base can be considered rigid in the low-frequency band. The thrust transmitted by the thrust bearing is transmitted to the hull through the oil film, and the transmission paths are parallel. It is logical that the longitudinal stiffness of the thrust bearing is equivalent to the longitudinal spring element with a single-DOF. However, when the thrust bearing is supported by an elastic support, the bearing shell and tile will move together with the vibration isolation system when the force of the vibration isolation system changes, resulting in an increase in the load of the thrust tile on one side of the deviating thrust disk, i.e., spring compression; a decrease in the load of the tile on the other side of the deviating thrust disk, i.e., spring elongation; and the unequal reaction of the two pairs of the thrust tile to the thrust disk

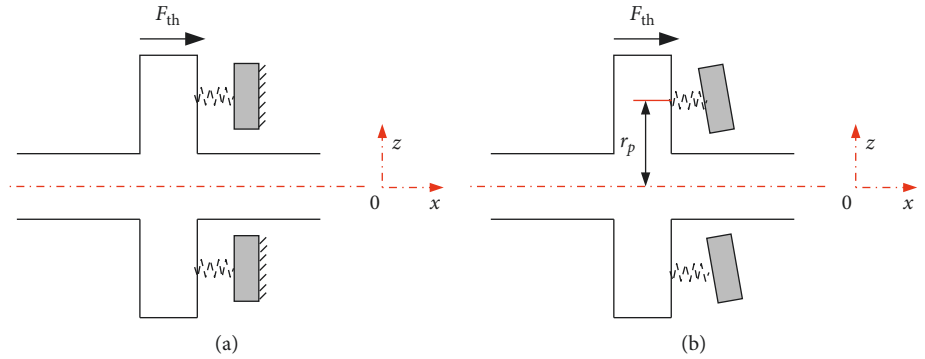

Figure 5: Two modeling methods of thrust bearing. (a) Single-DOF. (b) Multi-DOF.

will result in an increase in the load of the thrust disk. It is inaccurate to form an additional bending moment by using the single-DOF longitudinal spring element in its modeling, and the angular stiffness which characterizes the bending transfer relationship should also be taken into account.

The vertical transfer path of thrust bearing II (self-aligning thrust bearing) is mainly transmitted by the sealing elements at both ends of the bearing shell. Its 6-DOF expression is $K_{th} = \mathrm{diag}(k_{th-x}, k_{th-y}, k_{th-z}, 0, k_{th-\beta}, k_{th-\gamma})$, so its longitudinal bending transfer matrix is as follows:

$$T_{th-k} = \begin{bmatrix} 1 & \frac{1}{k_{th-x}} & & & & \\ 0 & 1 & & & & \\ & & 1 & 0 & 0 & -\frac{1}{k_{th-z}} \\ & & 0 & 1 & \frac{1}{k_{th-\beta}} & 0 \\ & & 0 & 0 & 1 & 0 \\ & & 0 & 0 & 0 & 1 \end{bmatrix}. \quad (7)$$

The bending stiffness is multiplied by the longitudinal stiffness of the symmetrical two equivalent springs by the square of the supporting position r_p of the tile, that is, $k_{th-\beta} = k_{th-x}/2 \times r_p^2$. The multi-DOF transfer matrix of equivalent mass and the spring element of the integral vibration isolation system is derived. As shown in Figure 6, the state vector transmitted to the mass element of thrust bearing II is Z^1, the state vector transmitted to the left end of the vibration isolation system is Z^2, the state vector transmitted to the spring element is Z^3, and the end is Z^4.

In the low-frequency band, the left displacement vector (2 points) and the right displacement vector (3 points) satisfy the rigid body kinematics based on the rigid body hypothesis:

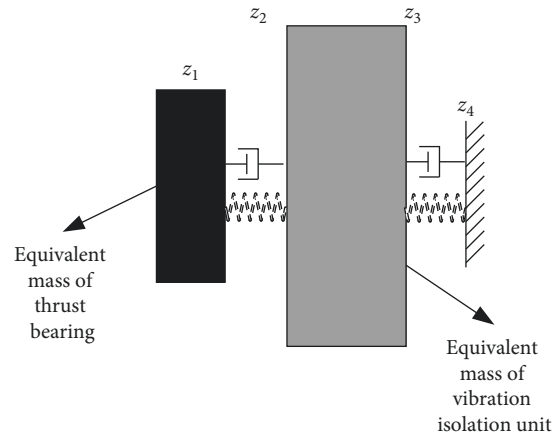

Figure 6: Local schematic diagram of the simplified model of thrust bearing, an IVIS.

$$x_3 = G_3 G_2^{-1} x_2, \quad (8)$$

where G_i $(i = 2, 3)$ is the coordinate matrix of the position transformation at the center of gravity of the vibration isolation system relative to the left access point 2 and the right output point 3, respectively. Two points correspond to the installation point of thrust bearing II on the intermediate raft body, and three points correspond to the center of mass of the vibration isolation system:

$$\begin{cases} x_3 = x_2 - z_{th}^0 \beta_2, \\ z_3 = z_2 + x_{th}^0 \beta_2, \\ \beta_3 = \beta_2. \end{cases} \quad (9)$$

At the same time, the force vectors of two and three points satisfy the classical dynamics theory:

$$F_3 = -\omega^2 \left(G_3^T\right)^{-1} M_{ivi} G_2^{-1} x_2 + \left(G_3^T\right)^{-1} G_2^T F_2. \quad (10)$$

Ignoring the inertia product in the mass matrix of the vibration isolation system, we can get that

$$\begin{cases} F_{3x} = -m_{ivi}\omega^2 x_2 + F_{2x} + m_{ivi}\omega^2 z_{th}^0 \beta_2, \\ F_{3z} = m_{ivi}\omega^2 z_2 + F_{2z} + m_{ivi}\omega^2 x_{th}^0 \beta_2, \\ M_{3y} = -I_{ivi-yy}\omega^2 \beta_2 + M_{2y} + z_{th}^0 F_{2x} + x_{th}^0 F_{2z}. \end{cases} \quad (11)$$

Formulas (10) and (11) are written in the form of transfer matrices:

$$T_{ivi-m} = \begin{bmatrix} 1 & 0 & 0 & -z_{\text{th}}^0 & 0 & 0 \\ -m_{ivi}\omega^2 & 1 & 0 & m_{ivi}\omega^2 z_{\text{th}}^0 & 0 & 0 \\ 0 & 0 & 1 & x_{\text{th}}^0 & 0 & 0 \\ 0 & 0 & 0 & 1 & 0 & 0 \\ 0 & z_{\text{th}}^0 & 0 & -I_{ivi-yy}\omega^2 & 1 & x_{\text{th}}^0 \\ 0 & 0 & m_{ivi}\omega^2 & m_{ivi}\omega^2 x_{\text{th}}^0 & 0 & 1 \end{bmatrix}. \quad (12)$$

Among them, x_{th}^0 and z_{th}^0 are the distance between the installation position of thrust bearing II and the center of gravity of the whole vibration isolation system. The three-DOF stiffness matrix of the overall vibration isolation system in the XOZ plane is as follows:

$$K_{ivi-k} = \begin{bmatrix} k_{ivi-x} & 0 & k_{ivi-x\beta} \\ 0 & k_{ivi-z} & k_{ivi-z\beta} \\ k_{ivi-x\beta} & k_{ivi-z\beta} & k_{ivi-\beta} \end{bmatrix}. \quad (13)$$

According to the force and deformation of the left and right ends of the spring element multiplied by the elastic coefficient equal to the action force, combined with the positive direction of the element coordinate system, it can be obtained that

$$\begin{bmatrix} k_{ivi-x} & 0 & k_{ivi-x\beta} \\ 0 & k_{ivi-z} & k_{ivi-z\beta} \\ k_{ivi-x\beta} & k_{ivi-z\beta} & k_{ivi-\beta} \end{bmatrix} \begin{bmatrix} x_{ivi-k}^R - x_{ivi-k}^L \\ z_{ivi-k}^L - z_{ivi-k}^R \\ \beta_{ivi-k}^R - \beta_{ivi-k}^L \end{bmatrix} = \begin{bmatrix} F_x \\ F_z \\ M_y \end{bmatrix}. \quad (14)$$

Based on the principle that the forces acting on the two ends of the spring element are equal, the longitudinal bending coupling transfer matrix in the vertical plane of the equivalent spring element of the whole vibration isolation system can be obtained:

$$T_{ivi-k} = \begin{bmatrix} 1 & \frac{k_{ivi-z}k_{ivi-\beta} - k_{ivi-z\beta}^2}{\Delta} & 0 & 0 & -\frac{k_{ivi-z} \times k_{ivi-x\beta}}{\Delta} & \frac{k_{ivi-x\beta} \times k_{ivi-z\beta}}{\Delta} \\ 0 & 1 & 0 & 0 & 0 & 0 \\ 0 & -\frac{k_{ivi-x\beta} \times k_{ivi-z\beta}}{\Delta} & 1 & 0 & \frac{k_{ivi-x} \times k_{ivi-z\beta}}{\Delta} & -\frac{k_{ivi-x}k_{ivi-\beta} - k_{ivi-x\beta}^2}{\Delta} \\ 0 & -\frac{k_{ivi-z} \times k_{ivi-x\beta}}{\Delta} & 0 & 1 & \frac{k_{ivi-x} \times k_{ivi-z}}{\Delta} & -\frac{k_{ivi-x} \times k_{ivi-z\beta}}{\Delta} \\ 0 & 0 & 0 & 0 & 1 & 0 \\ 0 & 0 & 0 & 0 & 0 & 1 \end{bmatrix}. \quad (15)$$

Among them, $\Delta = k_{ivi-x} \times k_{ivi-z} \times k_{ivi-\beta} - k_{ivi-z} \times k_{ivi-x\beta^2} - k_{ivi-x} \times k_{ivi-z\beta^2}$. After ignoring the factors of longitudinal and bending coupling of the shafting itself, it can be found that the main causes of the longitudinal bending coupling between the whole vibration isolation system and the shafting system are the asymmetry of the stiffness matrix and the vertical installation position coordinate z_{th}^0 of the thrust bearing relative to the center of gravity of the vibration isolation system, which are defined as the stiffness coupling and mass coupling, respectively.

The transfer relations of state vectors at both ends are as follows:

$$Z^R = T_{ivi-k} \times T_{ivi-m} \times T_{\text{th}-k} \times Z^L. \quad (16)$$

Among them, state vector $Z^i\,(i = R, L) = \begin{bmatrix} X & F_x & z & \beta & M_y & F_z \end{bmatrix}^T$ at both ends; the existing vessel generally adopts the integral vibration isolation system. The right end of the system is fixed. The constraint force of thrust bearing II simplified mass elements, namely, F_x^{II}, M_y^{II}, and F_Z^{II}, can be obtained:

$$\begin{cases} x^R = x^L, \\ F_x^R = F_x^L - m_{\text{th}}\omega^2 x^L - F_x^{\text{II}}, \\ z^R = z^L, \\ \beta^R = \beta^L, \\ M_y^R = M_y^L - J_{\text{th}}\omega^2 \beta^L - M_y^{\text{II}}, \\ F_z^R = F_z^L + m_{\text{th}}\omega^2 z^L - F_z^{\text{II}}. \end{cases} \quad (17)$$

Formula (17) is formulated as a matrix, which is the analytical expression of the modified bending longitudinal transfer matrix of the simplified mass element of the thrust

bearing. With this model, the natural vibration characteristics and forced vibration characteristics of the shafting with the elastic support can be calculated. When considering different directions of the supporting bearings, the aforementioned modeling method can still be extended to the horizontal bending vibration, where the state vectors at both ends are 10×1 column vectors and the transfer matrix is 10×10 matrix.

3. Experiment

It mainly includes the DC main propulsion motor (rated power 300 kW and speed 250 rpm), propulsion shafting, radial bearing, Michel thrust bearing, high elastic coupling, hull base, and auxiliary cooling and lubrication system. The stern end of the shafting is simulated by an external loading device to simulate the longitudinal excitation of the propeller. The test section can truly reflect the mechanical environment of the marine stern and can be used for noise reduction of marine machinery and equipment, dynamic characteristics of shafting rotor, and so on. It is a multifunctional platform for noise reduction of marine stern machinery.

3.1. Longitudinal Shafting Excitation System. The longitudinal shafting excitation system is loaded by the hydraulic servo system and controlled by force feedback. As shown in Figure 7, the system consists of articulated hinges, hydraulic cylinders, servo valves, force sensors, and rotating mechanism. The flow of hydraulic oil is controlled by servo valves, and then the loading force is controlled. The loading frequency is controlled by the switching frequency of servo valves. The internal disc spring and the thrust roller bearing in the rotating mechanism can be realized. The static force of −150 kN~150 kN and 10% dynamic force are loaded longitudinally, and the loading frequency ranges from 2.5 to 30 Hz.

3.2. Propulsion Shafting. Shaft system is composed of stern section, intermediate thrust shaft, and stern thrust shaft; each subsection shaft is connected by hinged bolts. Stern end is connected with flange of exciting equipment, and the stern end is connected with the output shaft of main propulsion motor through high elastic coupling; stern section is supported by two water-lubricated bearings, water supply pressure is about 0.3 MPa, and intermediate bearing is lubricated by natural lubrication, as shown in Figure 8.

Two thrust bearings are connected in series in the shaft system. Among them, thrust bearing I is installed in the conventional way, directly rigidly connected to the hull; thrust bearing II is installed on the intermediate raft by floating raft vibration isolation installation. During the experiment, the load-bearing switching between the two thrust bearings can be realized by manipulating the hydraulic hand-operated pump, and the effect of the floating raft vibration isolation system on the longitudinal vibration of the shafting can be verified by comparison.

4. Vibration Characteristics

As shown in Figure 9, there are five radial bearings in the bench shafting of the laboratory. They are stern rear bearing 1#, stern front bearing 2#, thrust bearing I front and rear bearing 3#, 4#, and intermediate bearing 5#. The radial bearings are simplified as single-point supporting spring elements, assuming that the stiffness of each direction is the same; considering the weight of the propeller, the support point of the stern rear bearing is 1/4 of the bush. The midpoint of the sleeve is used as the fulcrum position. The parameters of each bush are as follows: the diameter of rear stern bearing is 220 mm and the length is 650 mm; the diameter of front stern bearing is 220 mm and 730 mm; the diameter of thrust bearing I radial bush is 220 mm and 180 mm; and the diameter of intermediate bearing bush is 180 mm and 275 mm. The shafting is divided into 30 components with the length of 40 mm as the minimum component size.

Before analyzing the coupled vibration characteristics of the system, it is necessary to determine the support stiffness values of the radial bearings, which have a great influence on the bending vibration shape of the shafting. However, the radial bearings of marine shafting are hydrodynamic sliding bearings. Influenced by lubrication state, the installation position and alignment state of shafting, their mechanical characteristics are complex, often accompanied by obvious nonlinear characteristics, and engineering testing is difficult. In this section, Jasper's empirical formula for the numerical calculation of the stiffness of marine radial bearings is used to qualitatively analyze the changing trend of the bending vibration characteristics of thrust bearing II with elastic supports.

Empirical formula:

$$k_{rb} = \frac{cP}{\delta}. \tag{18}$$

Among them, c is the empirical coefficient, generally takes 2, P is the bearing load when the shaft system is in alignment, and δ is the radial clearance when each bearing is installed. Applying the shafting school transfer matrix model to calculate the bearing load, combined with the radial clearance of each bearing installation, the equivalent stiffness values of each bearing can be obtained, as shown in Table 1.

The above numerical results of radial bearing stiffness are substituted into the model, together with the longitudinal stiffness value of thrust bearing (1×10^9 N/m). Since the radial support stiffness of the seal assembly at both ends of self-aligning thrust bearing is difficult to determine, it is tentatively designated as 3×10^5 N/m. The unit force sweep frequency is applied at the propeller end, and the sweep frequency range is 0~100 Hz.

4.1. Comparing the Vibration Characteristics of Shafting under Two Kinds of Support Systems. The bending vibration characteristics of thrust bearings under two supporting conditions are summarized, as shown in Table 2.

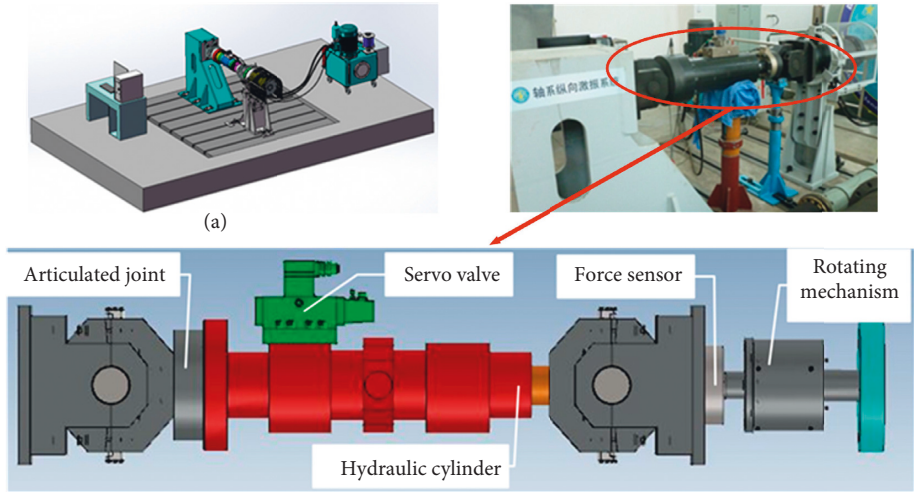

Figure 7: Axial excitation system. (a) Structural sketch. (b) Detail structure.

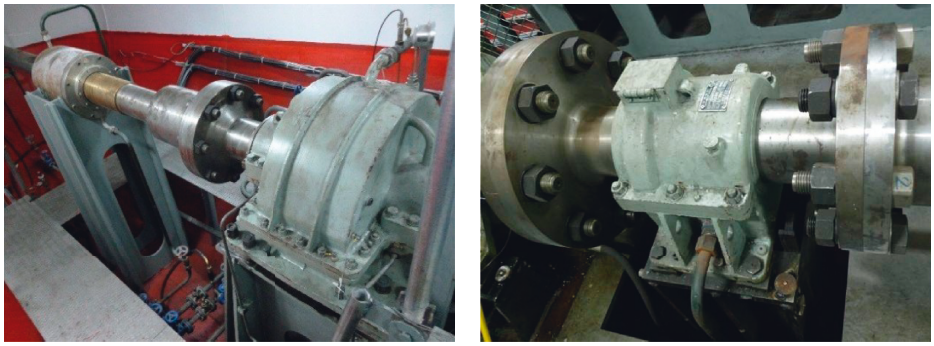

Figure 8: The physical picture of the shafting system.

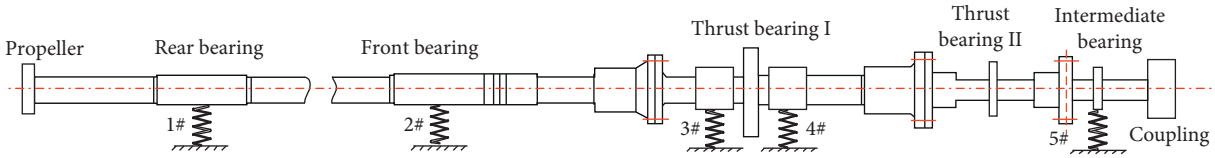

Figure 9: Schematic diagram of marine propulsion shafting.

Table 1: Related parameters of each radial bearing.

Num	1#	2#	3#	4#	5#
Load (kN)	44.75	57.48	49.95	84.27	55.98
Interval (mm)	1	1	0.3	0.3	0.2
Stiffness (N/m)	$8.95e^7$	$1.14e^8$	$3.33e^8$	$5.66e^8$	$5.60e^8$

From Figure 10 and Table 2, it can be seen that thrust bearings only have a great influence on the local bending vibration of shafting under the condition of an elastic support but have little influence on other bending modes. Observing Figures 10(d)–10(f), it can be seen that there are more chaotic peaks at about 10 Hz, which are mainly due to the mixing of three-DOF modes of the vibration isolation system: longitudinal 10.2 Hz, vertical 8.5 Hz, and pitch

Table 2: Comparison of bending characteristics of shafting under different supporting conditions of thrust bearing.

Number	Frequency (Hz)		Modal
	Rigid support	Elastic support	
①	13.9	13.9	First-order bending
②	43.7	45.1	Second-order bending
③	87.5	89.5	Third-order bending
④	50.5	73.0	Local bending

11.8 Hz. The corresponding frequency values of number 4 are substituted into the model, and the vertical dynamic deflections of each element are obtained. The corresponding local bending modes can be obtained after regularization, as shown in Figure 11.

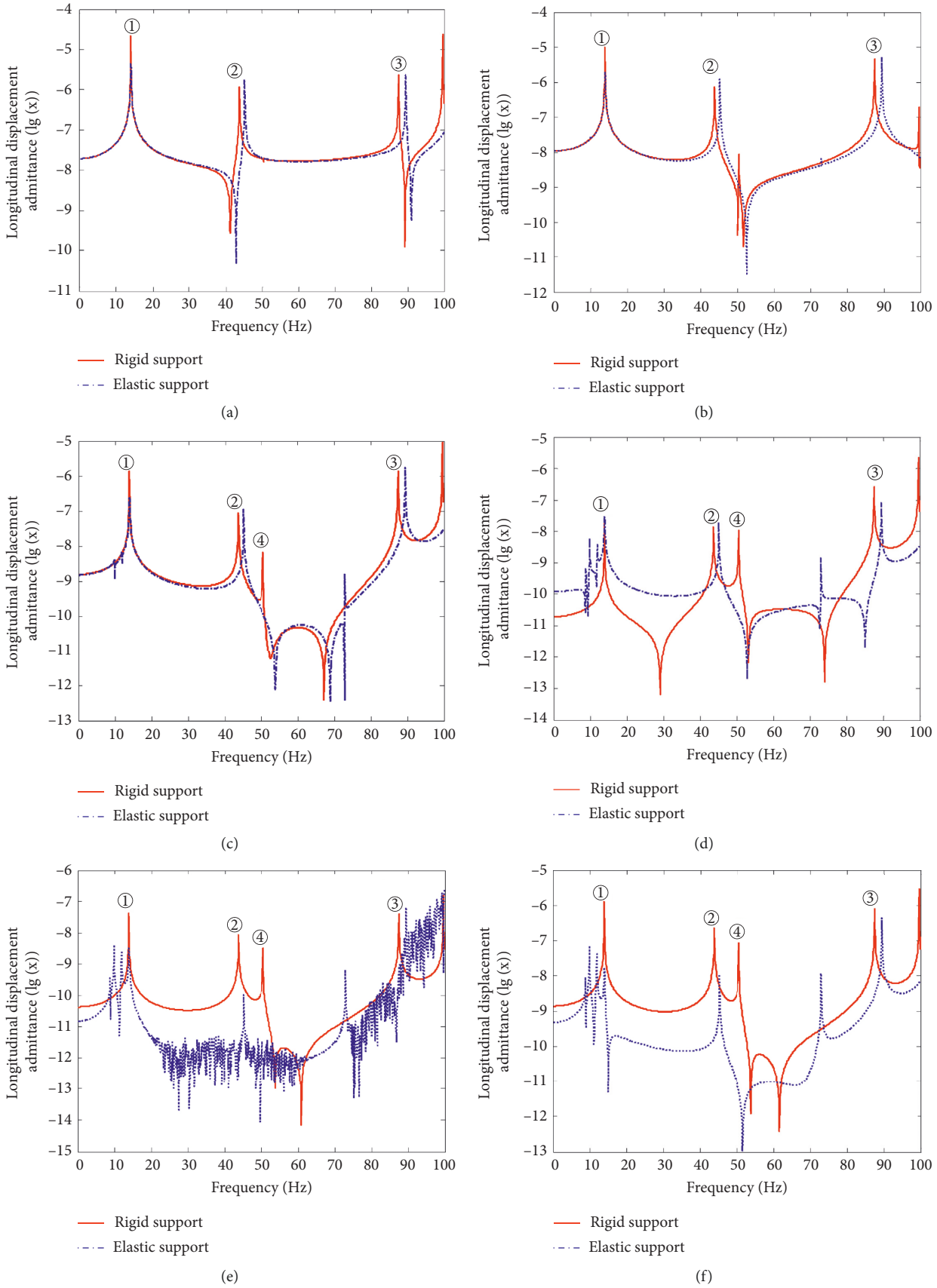

Figure 10: Vertical displacement admittance at each point of the coupling system. (a) 1#. (b) 2#. (c) 3#. (d) 4#. (e) 5#. (f) Thrust bearing II.

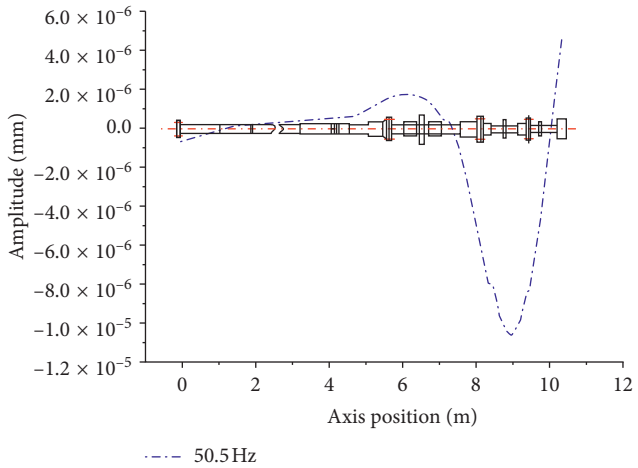

Figure 11: Local bending shape of shafting.

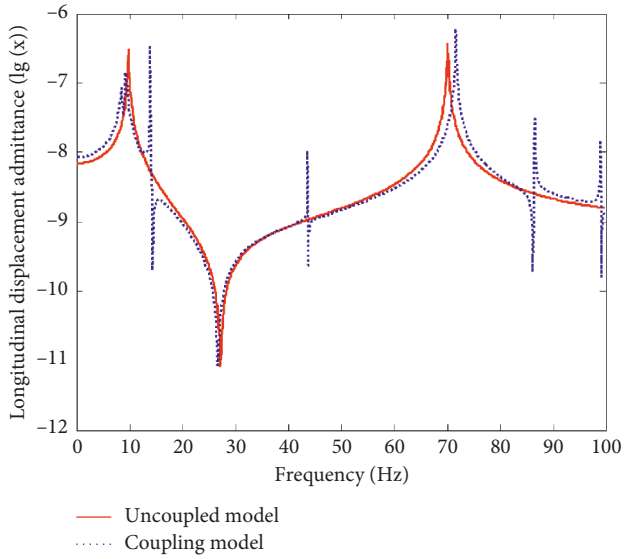

Figure 12: Longitudinal displacement admittance of thrust bearing with coupled effect or not.

In summary, although the radial bearing bush design of thrust bearing II has been cancelled, the stiffness characteristics of the vibration isolation system will affect the bending modes of shafting with thrust bearing II as the main vibration form and have little effect on other bending modes. That is to say, for the bending vibration of shafting, the vibration isolation system only affects the bending stiffness near the support, and the support will show coupling characteristics, that is, the inherent vibration characteristics of the vibration isolation system are mixed.

4.2. Comparison of Longitudinal Vibration Characteristics of Shafting under Two Kinds of Support Systems. The longitudinal displacement admittance curves of each point of the shafting are analyzed. It is pointed out that all points show the same vibration characteristics. The low-frequency band is similar to that of one-dimensional rod. The longitudinal displacement admittance curves at thrust bearings can be

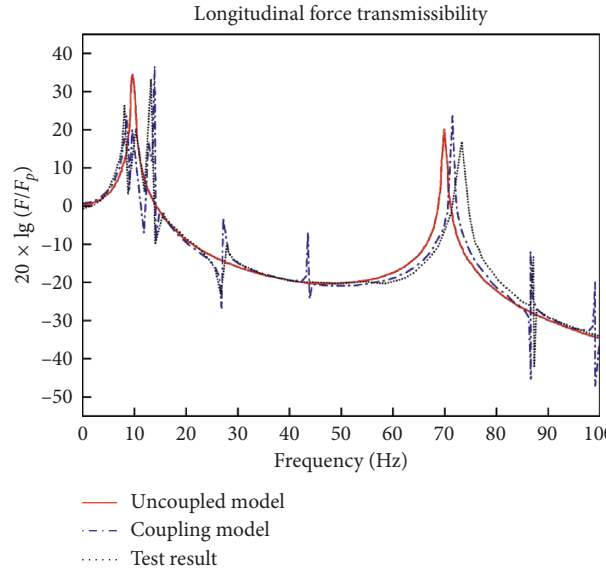

Figure 13: Longitudinal force transmissibility.

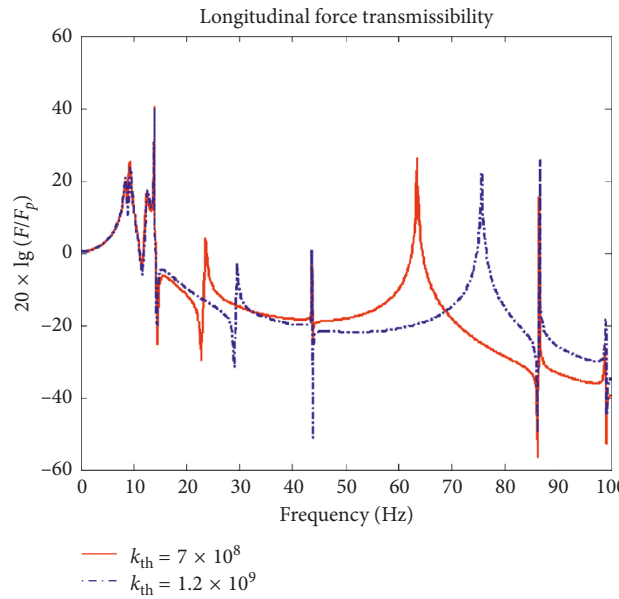

Figure 14: Longitudinal force transmissibility under different stiffness of thrust bearing.

used to qualitatively analyze the longitudinal vibration characteristics of the shafting. However, the influence of multi-DOF coupling is not considered when studying the elastic support of thrust bearings. Therefore, the longitudinal bending coupling model is used in this section to study the longitudinal vibration characteristics of thrust bearings II under single load, and the admittance curve at thrust bearings II is still used for qualitative analysis.

As can be seen from Figure 12, considering the multi-DOF coupling, the bending characteristic frequencies of shafting are found in the longitudinal displacement admittance curve of shafting, which accords with the general understanding of shafting vibration characteristics.

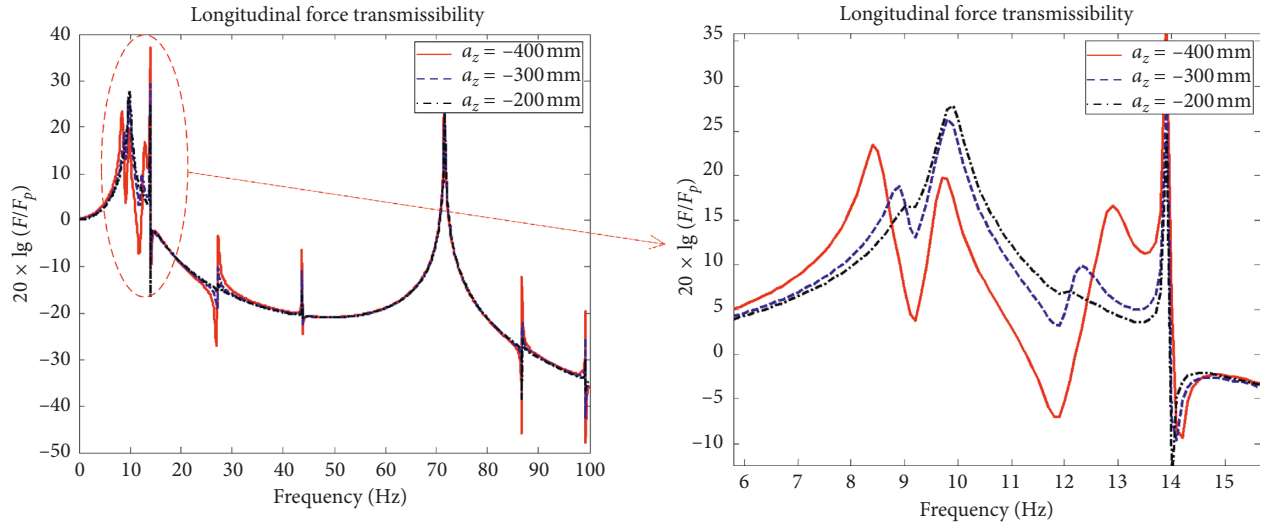

Figure 15: Longitudinal force transmissibility with different vertical arrangement a_z of isolators.

In summary, considering the multi-DOF coupling, the characteristic line spectra of the longitudinal vibration characteristics of shafting will appear to characterize the bending characteristics.

5. Transfer Characteristics

5.1. Longitudinal Transfer Characteristics. The whole vibration isolation system starts from the low-frequency vibration reduction of marine thrust bearings and pays more attention to the transmission characteristics of the longitudinal force in the low-frequency band. Formula (19) is still used to study the transmission characteristics T_f of the longitudinal force in the case of multi-DOF coupling. The parameters in formula (19) represent three-DOF matrices or vectors:

$$T_f = \frac{K_{ivi}K_{\text{th}}}{K_{\text{th}} + K_{ivi} - M_{ivi}\omega^2} \frac{x_{\text{th2}}}{F_p}. \tag{19}$$

Because of the lack of accurate numerical value of the propeller end force vector, the simulation is carried out under the assumption of $F_p = [1 \ 1 \ 1]^T$.

Figure 13 shows that compared with the test results, the coupling model has higher accuracy and can be used to analyze longitudinal force transmissibility. The longitudinal force transmissibility curve with multi-DOF coupling has more coupling frequencies: 8.5 Hz (vertical vibration of isolation system), 9.9 Hz (first-order longitudinal vibration of shafting), 12.6 Hz (pitching vibration of isolation system), 13.9 Hz (first-order bending vibration of shafting), 27.3 Hz (resonance frequency of thrust bearing), 43.7 Hz (second-order bending vibration of shafting), and 71.6 Hz (second-order longitudinal vibration of shafting). Although there are many coupling frequencies, only the first-order longitudinal vibration isolation system, the pitch of the isolation system, the first-order bending of the shafting system, and the second-order longitudinal vibration isolation of the shafting system have no effect on vibration reduction. The whole vibration isolation system at other coupling frequencies can still achieve thrust bearing vibration reduction. It should be noted that, except for the inevitable bending vibration frequency of shafting, the longitudinal vibration of the vibration isolation system is coupled with pitching, and the initial frequency of the vibration reduction band should consider pitching frequency.

Considering the influence of longitudinal stiffness of thrust bearings under different working conditions, the range of longitudinal stiffness ($7 \times 10^8 \sim 1.2 \times 10^9$ N/m) of thrust bearings under stealth working conditions is discussed.

Figure 14 shows that the longitudinal stiffness of the thrust bearing only affects the antiresonance frequency and the second-order natural frequency of the thrust bearing but has no effect on other frequencies. The main reason is that the large mass effect of the vibration isolation system weakens the interaction between the vibration isolation system and the shafting system. In fact, the first-order natural frequency of the shafting system is the longitudinal natural frequency of the vibration isolation system. The vertical installation position coordinate a_z of the isolator is the main reason for the non-decoupling of the midstiffness matrix. Therefore, a_z is chosen as −400 mm, −300 mm, and −200 mm, respectively, for simulation.

Figure 15 shows that reducing the vertical installation position coordinate a_z of the isolator is helpful to reduce the coupling effect of multi-DOF shafting. Therefore, in accordance with the characteristics of reducing displacement, the vertical installation position coordinate a_z of the isolator should be as close as possible to the center of gravity of the system in order to realize the stiffness matrix decoupling of the isolation system.

5.2. Vertical Transfer Characteristics. Based on the existing stiffness values of radial bearings, the transmission characteristics of vertical force of the propeller after elastic support of thrust bearings are qualitatively analyzed.

Figure 16 shows that compared with the test results, the coupling model has higher accuracy and can be used to

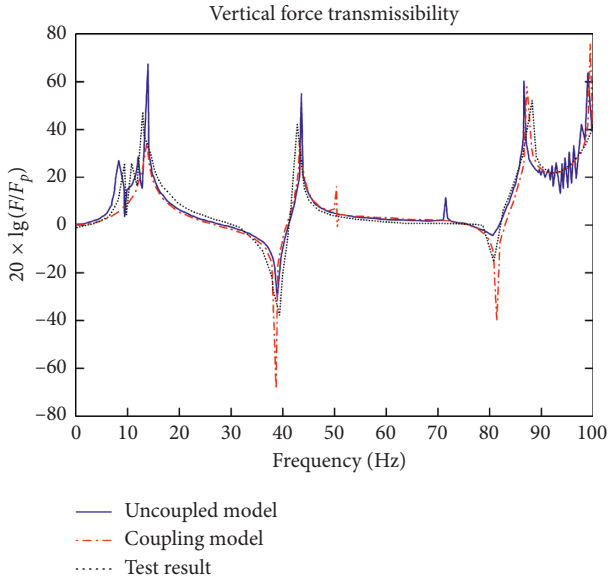

Figure 16: Vertical force transmissibility.

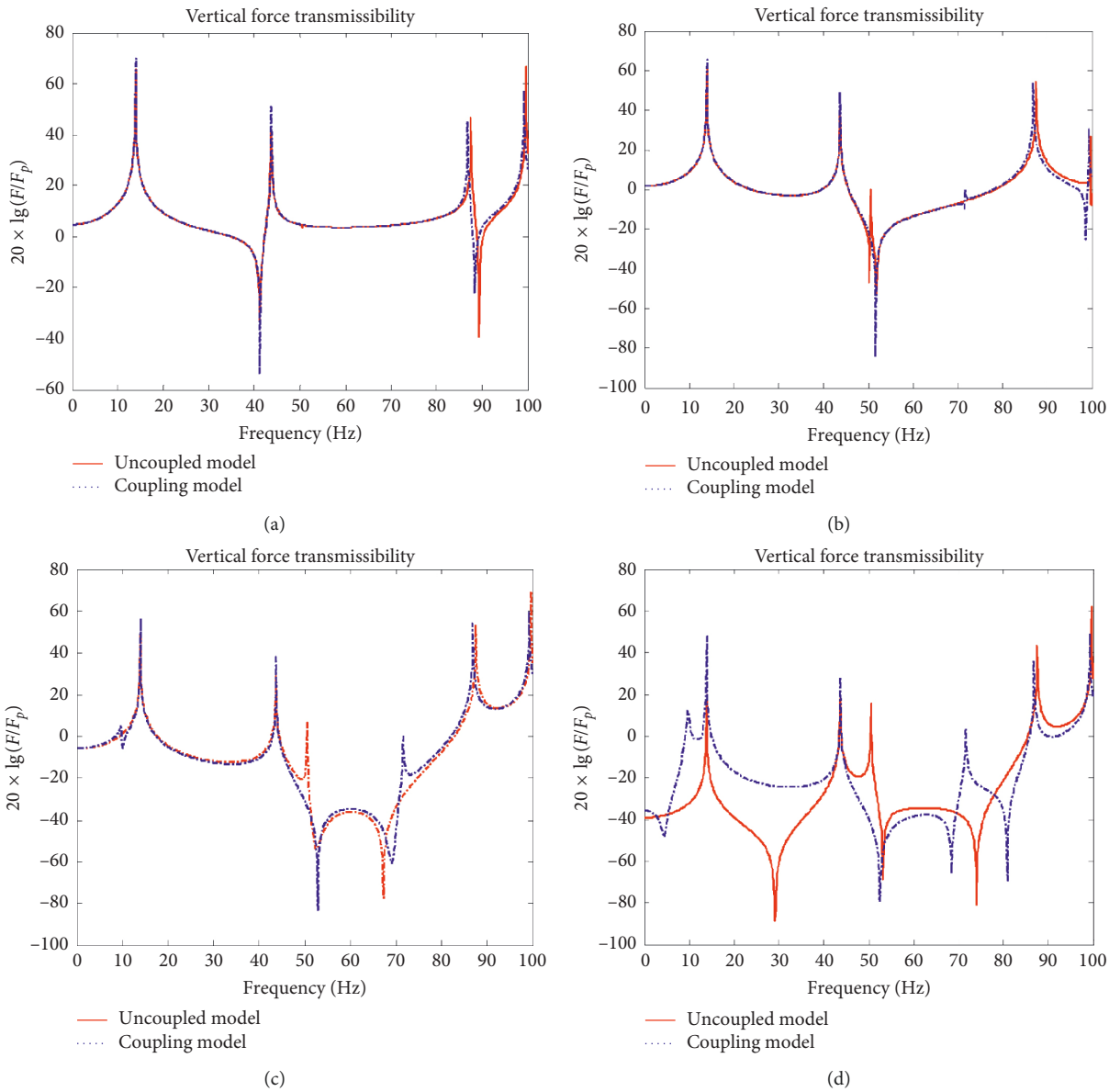

Figure 17: Continued.

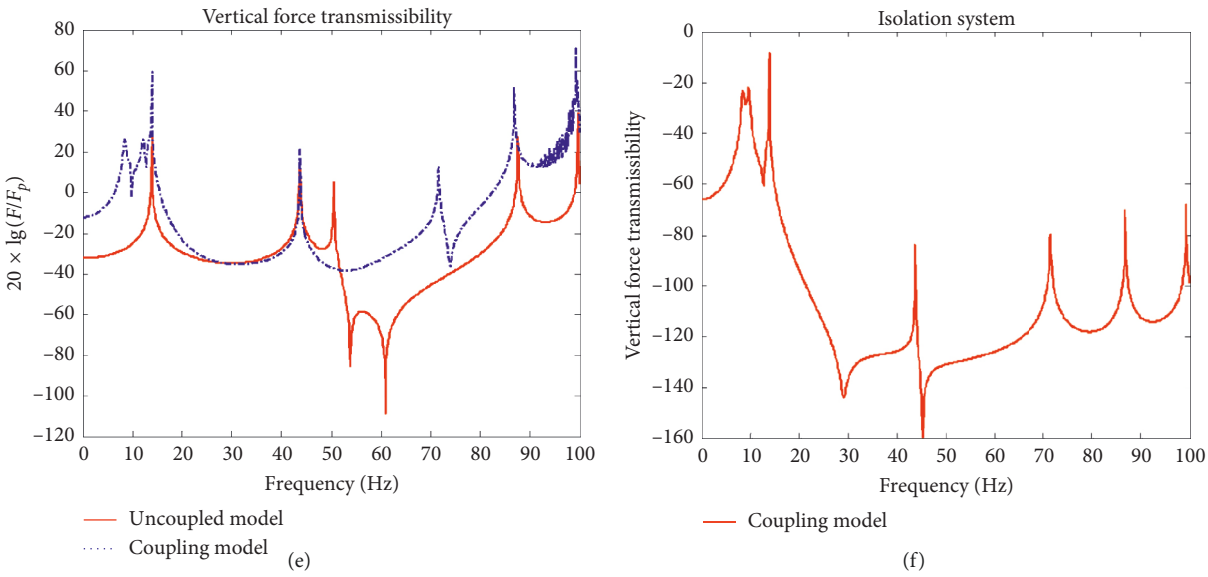

Figure 17: Vertical force transmissibility on every path. (a) 1#. (b) 2#. (c) 3#. (d) 4#. (e) 5#. (f) Isolation system.

analyze vertical force transmissibility. Compared with the uncoupled model, the vertical force transfer characteristics of thrust bearings with elastic supports do not change much in the low frequency, and there will be correlated frequencies showing the vibration form of the isolation system. It shows that the main influence on the local stiffness of thrust bearings is distributed in the high frequency. It is also necessary to analyze the components in the transmission path of the radial bearings with or without coupling.

Observing the vertical force transfer component on each transmission path in Figure 17, it can be found that the vertical force transmission characteristics of 1#, 2#, and 3# bearings are smaller in the coupled model and the uncoupled model. In 4#, 5# bearings, the vertical force characteristics are quite different, showing the coupling phenomenon of longitudinal vibration and bending vibration of the shafting, and the characteristic frequency which characterizes the vibration shape of the vibration isolation system appears. At the same time, the overall vibration isolation system is not rigid supported by the thrust bearing, and the vertical force is transmitted to the hull through the vibration isolation system, but the amplitude is small.

6. Conclusions

This paper studies the dynamic characteristics of thrust bearing shafting after the elastic support and draws the following conclusions:

(1) The elastic support of thrust bearings only changes the local bending stiffness of thrust bearings, which affects the bending characteristic frequencies of thrust bearings as the main vibration form and has little influence on other bending characteristic frequencies of shafting.

(2) After thrust bearings are supported by elastic supports, the vertical force transmission path of the propeller changes from the initial radial bearings to radial bearings and vibration isolation systems. The vertical force transmission characteristics of 1#, 2#, and 3# bearings are almost unaffected. Vertical force transmission characteristics of 4# and 5# bearings change a lot, showing the characteristics of coupling between longitudinal and bending of shafting. Also, the characteristic frequencies of vibration forms of isolation systems are shown.

(3) In the case of multi-DOF coupling, the characteristic line spectrum of propeller longitudinal force transfers the characteristic curve which characterizes the bending of shafting appears. Under different stiffness values of thrust bearings, only the second-order longitudinal natural frequency of shafting and the antiresonance frequency of thrust bearings are affected, but the low-frequency and high-efficiency vibration reduction of thrust bearings can still be achieved.

Data Availability

The data used to support the findings of this study are available from the corresponding author upon request.

Conflicts of Interest

The authors declare that there are no conflicts of interest regarding the publication of this paper.

Acknowledgments

This study was supported by the National Key Research and Development Program (no. HJ20182A030144).

References

[1] L. He, W. Xu, W. Bu, and L. Shi, "Dynamic analysis and design of air spring mounting system for marine propulsion system," *Journal of Sound and Vibration*, vol. 333, no. 20, pp. 4912–4929, 2014.

[2] Z. Hu, L. He, W. Xu et al., "Optimization design of resonance changer for marine propulsion shafting in longitudinal vibration," *Chinese Journal of Ship Research*, vol. 14, no. 1, pp. 107–113, 2019.

[3] J. Plunt, "Finding and fixing vehicle NVH problems with transfer path analysis," *Sound and Vibration*, vol. 39, no. 11, pp. 12–16, 2005.

[4] G.-p. Feng, Y. Chen, and X. c. Huang, "Study on transmission paths in submarine stern excited longitudinally," *Noise and Vibration Control*, vol. 6, pp. 132–135, 2009.

[5] J. Pan, N. Farag, T. Lin et al., "Propeller induced structural vibration through the thrust bearing," in *Proceedings of the 2002 Innovation in Acoustics and Vibration Annual Conference of the Australian Acoustics Society*, pp. 390–399, Adelaide, Australia, November 2002.

[6] J. R. Xie, S. G. Sheng, and Y. S. Wu, "Transmission character of propeller excitation through shaft-line system to hull," *Shipbuilding of China*, vol. 52, no. 1, pp. 80–89, 2011, in Chinese.

[7] G. B. Zhang and Y. Zhao, "Elastic wave analysis on longitudinal vibration of marine propulsion shafting," *Shipbuilding of China*, vol. 153, no. 3, pp. 140–150, 2012, in Chinese.

[8] G. B. Zhang, Y. Zhao, T. Li, and X. Zhu, "Propeller excitation of longitudinal vibration characteristics of marine propulsion shafting system," *Shock and Vibration*, vol. 2014, Article ID 413592, 19 pages, 2014.

[9] Y. Zhao, G. B. Zhang, and L. Li, "Review of advances on longitudinal vibration of vessel propulsion shafting and control technology," *Shipbuilding of China*, vol. 52, no. 4, pp. 259–269, 2011.

[10] P. Lu, Y. Zhao, G. Zhang et al., "Development of experimental rig for marine propulsion shafting and longitudinal vibration characteristic test," *Journal of Vessel Mechanics*, vol. 17, no. 3, pp. 277–287, 2013.

[11] D.-L. Li, Y. Chen, Z.-y. Zhang, and H.-x. Hua, "Influence of thrust bearing's oil film stiffness on the coupled vibration of the shafting—vessel hull structure," *Noise and Vibration Control*, vol. 6, pp. 81–85, 2011.

[12] Z.-r. Yang, C.-y. Qin, Z.-s. Rao, and N. Ta, "Design and analysis of a dynamic absorber for reducing axial vibration of vessel shafting," *Journal of Vibration and Shock*, vol. 31, no. 16, pp. 48–61, 2012.

[13] C.-y. Qin, Z.-r. Yang, Z.-s. Rao, and N. Ta, "Study on suppression of the longitudinal vibration of vessel's propulsion shafting system," *Noise and Vibration Control*, vol. 33, no. 3, pp. 147–152, 2013.

[14] D. J. Mead and Y. Yaman, "The harmonic response of uniform beams on multiple linear supports: a flexural wave analysis," *Journal of Sound and Vibration*, vol. 141, no. 3, pp. 465–484, 1990.

[15] D. J. Mead and Y. Yaman, "The response of infinite periodic beams to point harmonic forces: a flexural wave analysis," *Journal of Sound and Vibration*, vol. 144, no. 3, pp. 507–529, 1991.

[16] R. J. Zhou and G. W. Yi, "Calculation method of vessel propulsion shafting longitudinal vibration and influencing factors," *Chinese Journal of Vessel Research*, vol. 6, no. 6, pp. 17–22, 2011.

[17] D. Zou, Z. Rao, and N. Ta, "Coupled longitudinal-transverse dynamics of a marine propulsion shafting under super-harmonic resonances," *Journal of Sound and Vibration*, vol. 346, pp. 248–264, 2015.

[18] D.-L. Zou, N. Ta, H. Zhu, K. Lu, Z.-L. Xie, and Z.-S. Rao, "Experiment of oil-film stiffness and composite support stiffness of thrust bearing in marine propulsion shafting," *Journal of Ship Mechanics*, vol. 21, no. 4, pp. 455–463, 2017.

[19] J. Y. He, L. He, W. Xu, and Z. M. Li, "Research on longitudinal vibration isolation of marine shafting under elastic supporting forms of thrust bearing," *Journal of Ship Mechancis*, vol. 21, no. 5, pp. 613–620, 2017.

[20] X. Q. Zhao, W. Xu, C. Shuai, and Z. c. Hu, "Research on dynamic characteristics of motor vibration isolation system through mechanical impedance method," *IOP Conference Series: Materials Science and Engineering*, vol. 274, Article ID 012051, 2017.